



Micropollutant Oxidation Studied by Quantum Chemical Computations

Methodology and Applications to Thermodynamics, Kinetics, and Reaction Mechanisms

Tentscher, Peter Rudolf; Lee, Minju; von Gunten, Urs

Published in:

Accounts of Chemical Research

DOI (link to publication from Publisher):

[10.1021/acs.accounts.8b00610](https://doi.org/10.1021/acs.accounts.8b00610)

Publication date:

2019

Document Version

Accepted author manuscript, peer reviewed version

[Link to publication from Aalborg University](#)

Citation for published version (APA):

Tentscher, P. R., Lee, M., & von Gunten, U. (2019). Micropollutant Oxidation Studied by Quantum Chemical Computations: Methodology and Applications to Thermodynamics, Kinetics, and Reaction Mechanisms. *Accounts of Chemical Research*, 52(3), 605-614. <https://doi.org/10.1021/acs.accounts.8b00610>

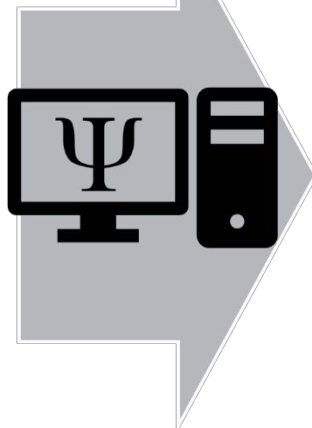
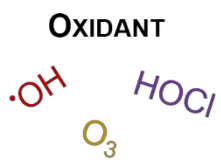
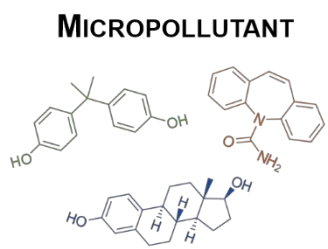
General rights

Copyright and moral rights for the publications made accessible in the public portal are retained by the authors and/or other copyright owners and it is a condition of accessing publications that users recognise and abide by the legal requirements associated with these rights.

- Users may download and print one copy of any publication from the public portal for the purpose of private study or research.
- You may not further distribute the material or use it for any profit-making activity or commercial gain
- You may freely distribute the URL identifying the publication in the public portal -

Take down policy

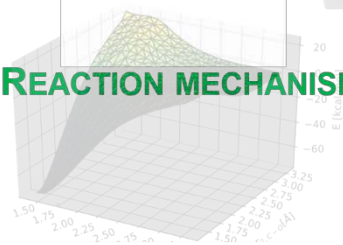
If you believe that this document breaches copyright please contact us at vbn@aub.aau.dk providing details, and we will remove access to the work immediately and investigate your claim.



REACTION KINETICS

THERMODYNAMICS

REACTION MECHANISMS



16

17 **CONSPECTUS**

18 The abatement of organic micropollutants during oxidation processes has become an
19 emerging issue for various urban water systems such as drinking water, wastewater
20 and water reuse. Reaction kinetics and mechanisms play an important role in terms of
21 efficiency of these processes and the formation of transformation products, which are
22 controlled by functional groups in the micropollutants and the applied oxidants. So
23 far, the kinetic and mechanistic information of the underlying reactions was obtained
24 by experimental studies, additionally, predictive quantitative structure activity
25 relationships (QSARs) were applied to determine reaction kinetics for the oxidation of
26 emerging compounds. Since this experimental approach is very laborious and there
27 are tens of thousands potential contaminants, alternative strategies need to be
28 developed to predict the fate of micropollutants during oxidative water treatment. Due
29 to significant developments in quantum chemical (QC) computations in recent years
30 and increased computational capacity, QC-based methods have become an alternative
31 or a supplement to the current experimental approach.

32

33 This article provides a critical assessment of the current state-of-the-art of QC-based
34 methods for the assessment of oxidation of micropollutants. Starting from a given
35 input structure, QC computations need to locate energetic minima on the potential
36 energy surface (PES). Starting from these minima, useful thermodynamic and kinetic
37 information can be estimated by different approaches: Experimentally determined
38 reaction mechanisms can be validated by identification of transition structures in the
39 PES, which can be obtained for addition reactions, heavy atom transfer (Cl^+ , Br^+ , O^+)
40 and H-atom transfer (simultaneous proton and electron transfer) reactions. However,
41 transition structures in the PES cannot be obtained for e^- -transfer reactions (SI, Text
42 S8).

43 Second order rate constants k for the reactions of micropollutants with chemical
44 oxidants can be obtained by *ab initio* calculations or by quantitative structure activity
45 relationships (QSARs) with various QC descriptors. It has been demonstrated that
46 second order rate constants from *ab initio* calculations are within factors 3-750 of the
47 measured values, whereas LFER-based methods can achieve factors 2-4 compared to
48 the experimental data. The orbital eigenvalue of the highest occupied molecular

49 orbital (E_{HOMO}) is the most commonly used descriptor for LFER-based computations
50 of k -values.

51 In combination with results from experimental studies, QC computations can also be
52 applied to investigate reaction mechanisms for verification/understanding of oxidative
53 mechanisms, calculation of branching ratios or regioselectivity, evaluation of the
54 experimental product distribution and assessment of substitution effects. Furthermore,
55 other important physical-chemical constants such as unknown equilibria for species,
56 which are not measurable due to low concentrations or $\text{p}K_{\text{a}}$ values of reactive
57 transient species can be estimated. With further development of QC-based methods, it
58 will become possible to implement kinetic and mechanistic information from such
59 computations in *in silico* models to predict oxidative transformation of
60 micropollutants. Such predictions can then be complemented by tailored experimental
61 studies to confirm/falsify the computations.

62

63 **INTRODUCTION**

64 ***Reactions of chemical oxidants with micropollutants***

65 Chemical oxidants (e.g., chlorine, ozone, chlorine dioxide, etc.) have been applied in
66 water treatment since more than a century, first for disinfection and later for
67 micropollutant abatement.¹ Chemical oxidants react mainly with water matrix
68 components such as the dissolved organic matter (DOM),¹ however in this article, we
69 will focus on the oxidative abatement of micropollutants, which has become a major
70 issue for drinking water, in water reuse systems, and enhanced municipal wastewater
71 treatment systems.¹ Typically, oxidation does not lead to a complete mineralization of
72 target micropollutants but to transformation products with initially similar structures
73 as the parent compounds.¹ Biologically active target compounds are inactivated by
74 these relatively minor changes in their molecular structures.¹ For extended oxidation
75 of micropollutants low molecular weight compounds will be formed, with limited or
76 no structural similarities to the target compounds, which may be of toxicological
77 concern.¹

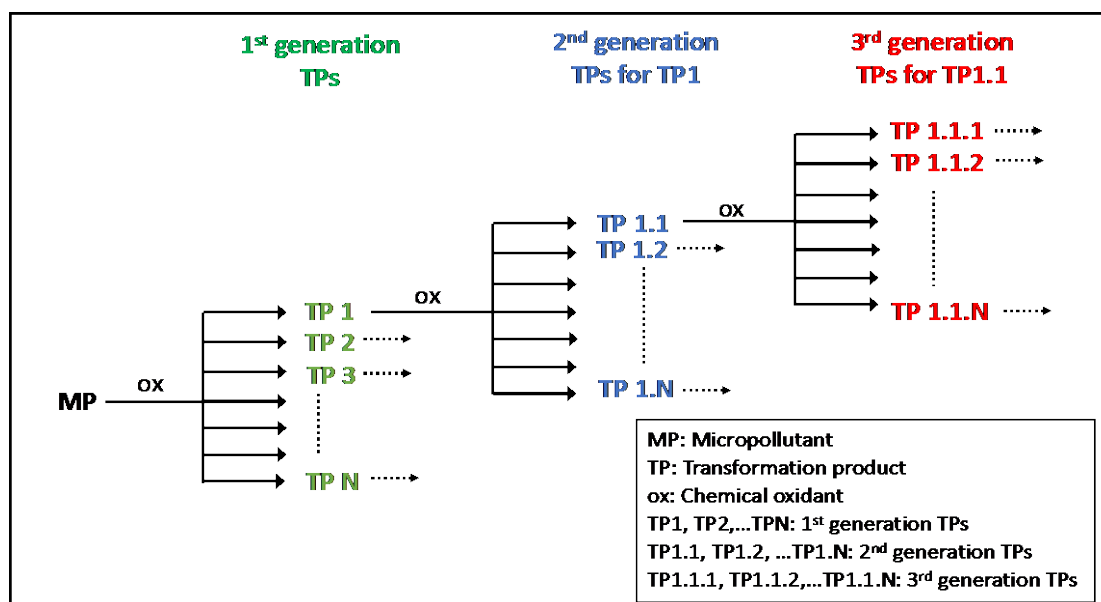
78 ***Assessment of oxidation processes***

79 So far, the efficiency of oxidation processes has been mainly assessed experimentally.
80 There is a large body of information on the kinetics and mechanisms of the reactions
81 of functional groups and micropollutants with chemical oxidants.¹ However, a purely

82 experimental approach for kinetic and mechanistic studies is labor-intensive and time
83 consuming. If only a fraction of the about 100'000 commercially available chemicals
84 can be found in water treatment systems (especially wastewater and water reuse), it
85 will be almost impossible to determine reaction kinetics, mechanisms and
86 transformation products experimentally (Figure 1).¹

87

88



90

91 Figure 1. Reactions of chemical oxidants with synthetic organic compounds (MPs). A
92 simplified reaction scheme illustrates the complexity for the formation of TPs.

93 Dashed arrows: Analogous reactions to TP1, TP1.1 and TP1.1.1 (not shown).

94

95 Rather, a focus on fundamental kinetic and mechanistic aspects with the main
96 oxidant-reactive functional groups is promising. This knowledge can then be
97 extrapolated to realistic systems to assess transformation product formation based on
98 the knowledge of functional groups of the reaction targets.¹

99

99 *Predictive methods for oxidation kinetics and mechanisms*

100 It is evident that prognostic tools are needed to estimate kinetic parameters and
101 determine mechanisms for oxidant-target compound reactions for the huge number
102 compounds.

103 *Reaction kinetics*

104 Second-order rate constants for the reactions of organic compounds with oxidants
105 such as hydroxyl radical, ozone, chlorine, bromine, chlorine dioxide, ferrate(VI) and
106 permanganate have been experimentally determined and compiled.²⁻⁹ Based on this
107 information, second-order rate constants for the reactions of emerging compounds
108 with oxidants can be estimated by quantitative structure activity relationships
109 (QSAR). This approach has been successfully applied for activated aromatic
110 compounds, olefins and amines for the oxidants ozone, chlorine, chlorine dioxide and
111 ferrate(VI) with Hammett and Taft sigma coefficients.¹⁰ Overall, predicted second-
112 order rate constants within a factor of 1/3-3 of the measured values can be obtained,
113 similar to the margin of different experimental studies. However, for complex
114 chemical structures, Hammett or Taft coefficients are sometimes difficult to obtain.¹⁰
115 Furthermore, second-order rate constants for the reactions of hydroxyl radical with
116 organic compounds have been estimated by the group contribution method.¹¹ The
117 advent of modern quantum chemical (QC) methodologies (e.g., density functional
118 theory, DFT) and the high-performance computing provided an affordable means for
119 theoretical investigations on oxidative reactions. Therefore, an alternative for
120 estimating second-order rate constants is based on QC computations (see below).¹²
121 This approach has the advantage that it is independent of Hammett or Taft sigma
122 values, which are not available for all chemical structures.

123 *Reaction mechanisms*

124 Transformation pathways during oxidative treatment of micropollutants can be
125 determined by labor-intensive experiments by analyzing transformation products by a
126 suite of analytical tools.¹ Such information has been applied to build computer-
127 assisted pathway prediction systems based on reaction rules for ozone and hydroxyl
128 radical.¹³⁻¹⁴ For other oxidants applied in water treatment (e.g., chlorine, chlorine
129 dioxide, permanganate, etc.), no comprehensive compilations of mechanistic
130 information are available and it is more difficult to predict reaction products.
131 Generally, the uncertainty of predictions increases with the extent of transformation
132 of the target compound, i.e., from the first-generation products to higher generation
133 products (Fig. 1). Based on the reaction mechanisms provided in literature, it is often
134 difficult to judge the likelihood of specific reactions among multiple pathways.
135 It has been demonstrated, that QC computations can complement or even substitute
136 experimental kinetic and mechanistic studies on the oxidation of organic
137 compounds.¹⁵⁻¹⁶ The goals of this paper are to (i) discuss the state-of-the-art of QC

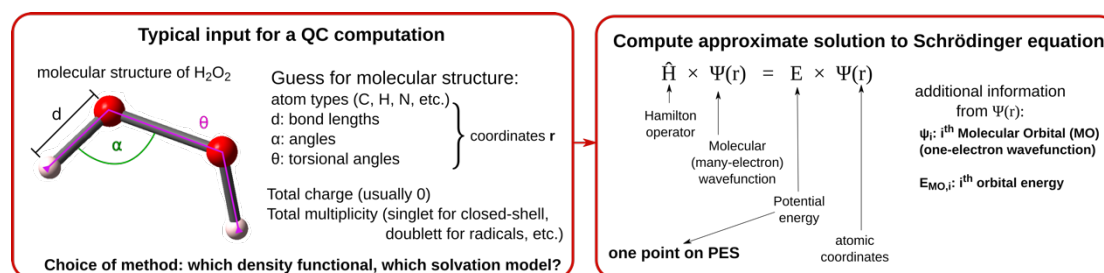
138 computations for oxidative processes, (ii) give examples and a critical evaluation of
139 the work that has been performed in this field, and (iii) assess the practical
140 implications of this approach.

141 QUANTUM CHEMICAL COMPUTATIONS: STATE-OF-THE-ART

142 General considerations

143 QC computations¹⁷ simulate isolated molecules or complexes, as opposed to a
144 solution containing molecules in high numbers. A typical input file and output is
145 exemplified in Figure 2.

146

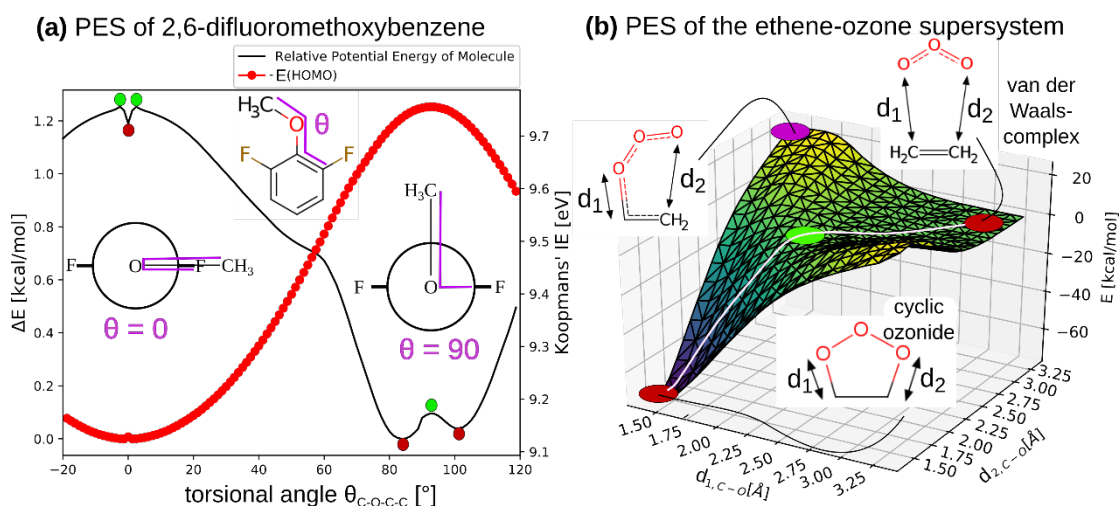


148 Figure 2: Required input for a QC computation and resulting information.

149

150 The approximate solution of the time-independent electronic Schrödinger equation
151 depends on the atomic coordinates r (bond lengths, angles, and torsional angles) as
152 parameters only (Born-Oppenheimer approximation) and yields the potential energy E
153 for a given set of coordinates (Figure 2). These $3N-6$ degrees of freedom (N =number
154 of atoms) define a potential energy surface (PES, Figure 3). The reactant and product
155 species of a reaction are defined by differences in r only, and the number of atoms has
156 to remain balanced for calculation of energy differences. From a given input structure,
157 a computer program will find the closest energetic minima (stationary structures) on
158 the PES, corresponding to observable chemical species. Based on this, further
159 analyses can lead to information on kinetics, thermodynamics, and reaction
160 mechanisms, which is elucidated in Figure 4.

161



162

163 Figure 3: The 3N-6-dimensional PES can be collapsed to one or two dimensions by
 164 systematically varying *one or two coordinates*, and optimizing the rest of the system.

165 (a) *Dihedral angle* of the $H_3C-O-C-CF$ torsion of 2,6-difluoromethoxybenzene (b)

166 *Two r_{C-O} distances* of the O_3 -ethene supersystem. Minima on the PES are marked in

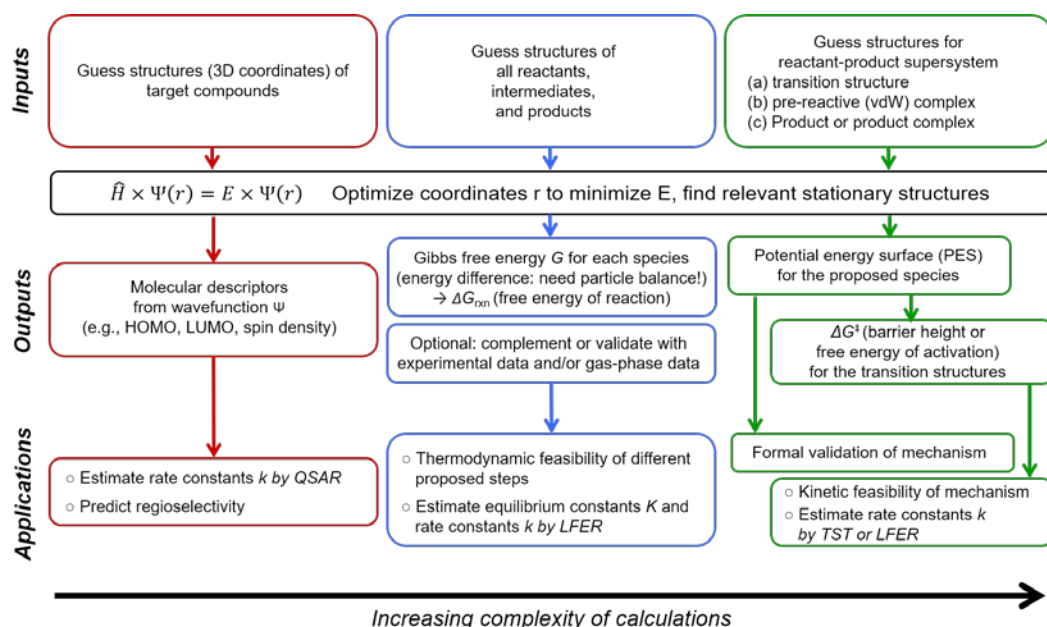
167 red, the transition structure connecting the minima in green. (b) also shows the

168 potential structure for a monodentate adduct (purple) and the minimum energy

169 path/“reaction coordinate” connecting reactants and products in white (computational

170 details: Supporting Information(SI) Text S7).

171



172

173 Figure 4: Calculation schemes with various complexities for obtaining the relevant

174 QC parameters of different applications as discussed in the manuscript. LFER: Linear

175 free energy relationship, TST: Transition state theory

176

177 **Evaluation of ΔG_{rxn} (thermodynamic feasibility and equilibria)**

178 Gibbs free energy (G or free energy hereafter) can be used to evaluate thermodynamic
179 feasibility or equilibria of a reaction (Figure 4, middle). This is implemented
180 following the thermodynamic cycle summarized in eq. (1), yielding the aqueous free
181 energy of reaction ΔG_{rxn} .

182
$$\Delta G_{\text{rxn}} = \sum G_{\text{products,gas}} + \sum \Delta G_{\text{products,solv}} - \sum G_{\text{reactants,gas}} - \sum \Delta G_{\text{reactants,solv}} \quad (1)$$

183 Only structures of individual species need to be provided, and can usually be easily
184 proposed. Moreover, the computation can be divided into a gas phase component and
185 a free energy of solvation ΔG_{solv} ,¹⁸ allowing for the use of highly accurate methods
186 (e.g., coupled cluster¹⁹) or experimental values for gas phase ΔG_{rxn} . The accuracy of
187 such calculations strongly depends on the model chemistry used for both the gas
188 phase and the solvation parts.

189 For gas phase energetics, the “gold standard” CCSD(T) method¹⁹ (SI, Text S1) can
190 achieve an accuracy of 1 kcal/mol (\cong experimental accuracy) for many problems of
191 organic chemistry, and should be used whenever affordable. Table 1 illustrates that
192 the uncertainty in thermodynamic properties stems primarily from the solvation
193 model, especially for ionic compounds. However, for some of the primary and
194 secondary oxidants bearing “multireference character” (including Cl_2O ,²⁰ ClO_2 ,²⁰
195 O_3 ,²¹ O_3^- , and $^1\text{O}_2$),²¹ and any singlet diradical intermediates (SI, Text S9), gas phase
196 results alone may already be equally uncertain. For example, free energy calculations
197 involving O_3 as a reactant suffer from a systematic error in ΔG_{rxn} of ~ 4 kcal/mol in the
198 gas phase electronic energy component when computed by CCSD(T), and even worse
199 with contemporary DFT methods.²¹ More sophisticated methods are necessary to
200 reach 1 kcal/mol accuracy,^{19, 21} which are not affordable for any target compounds of
201 interest. Careful method evaluation using smaller model compounds can be used to
202 select methods with reasonable results for real systems (SI, Text S1 for a discussion
203 of accuracy versus computer time).

204 In many difficult cases, lacking thermodynamic data can be compiled from
205 experimental data. Gas phase reaction energies, but also experimental $\text{p}K_{\text{a}}$ values,
206 redox potentials, or other equilibrium constants (linked to free energy differences
207 through $\log(K) = \Delta G/RT$) can be used in thermodynamic cycles to estimate desired
208 free energy differences or free energies of solvation needed for aqueous phase
209 calculations. This requires that the other components of the thermodynamic cycle are

210 computed close to experimental accuracy. Table 1 provides some examples of
211 achievable accuracies for such thermochemical simulations.

212

213 Table 1: Typically achievable average accuracies for thermodynamic parameters from

214 QC computations.^a

Thermodynamic parameter	Accuracy
ΔG_{rxn} (gas phase)	CCSD(T)/composite: ~1-2 kcal/mol ¹⁹ (~4 kcal/mol) ^{d21} DFT: 2-4 kcal/mol ²⁴
ΔG_{solv} (neutral species)	Implicit solvation: ^d 1-2 kcal/mol ²⁵
ΔG_{solv} (ionic species)	Implicit solvation: ^d 3-7 kcal/mol ²⁵
$\text{p}K_{\text{a}}$	Implicit solvation only: ^d ~6 pH units ²⁶ Implicit solvation with some explicit water molecules: ^e ~1 pH unit ²⁶
IE (gas) ^b	CCSD(T)/composite: ~1-2 kcal/mol ²⁷⁻²⁸ DFT: ~3-5 kcal/mol ²⁸
ΔG^{oc}	Implicit solvation: ^d ~0.3 V (~7 kcal/mol) ²⁹ Explicit solvation: ^d ~0.2 V (~4 kcal/mol) ³⁰

215 ^aResults should be compared to experimental data of similar systems (e.g.,
216 equilibrium constants of halogen oxides²²), or can be correlated to experimental data
217 of a congeneric series (e.g., one-electron oxidation potentials of anilines²³ see SI, Text
218 S1)

219 ^bgas phase adiabatic ionization energy

220 ^chalf-cell standard reduction potential

221 ^dreduced accuracy for multi-reference species

222 ^eSI, Text S2 for details on implicit and explicit solvation

223

224 **Computational validation of proposed reaction mechanisms**

225 For further mechanistic validation, stationary structures on the PES of combined
226 reactants need to be identified: (a) The pre-reactive complex of the reactants, (b) the
227 product (complex), and (c) a transition structure (first order saddle point on the PES)
228 connecting the reactant with the product side through a minimum energy path (Figure
229 3b).

230 This is possible if the minimum energy path can be easily expressed by atomic
231 coordinates (e.g., by one or two interatomic distances). However, oxidants react by
232 different mechanisms including electron transfer (ET) (Table 2) or variations thereof,
233 where transition structures cannot be identified like this (Table 3).

234 When describing bond formation/cleavage, common QC methods suffer from a poor
235 description of largely elongated bonds,^{17, 19} resulting in inaccurate energetics, and in
236 the worst case in qualitative differences in the PES described by different methods
237 (SI, Text S3). Such extreme problems should only arise when a molecular diradical is
238 involved.

239 Frequently, the initial reaction of an oxidant with a target compound will not lead to
240 the experimentally observed “primary” product, but to metastable intermediate(s) that
241 cannot be observed experimentally (Figure 1). However, only computing a complete
242 pathway from reactant to product can support a proposed reaction mechanism, which
243 can be quite laborious. Computed ΔG^\ddagger (barrier height or free energy of activation) can
244 be used as an additional criterion concerning the kinetic feasibility of a computed
245 mechanism, and can provide some insight into the kinetic control of the formation of
246 possible products.

247

248 Table 2: Common oxidants in water treatment and the corresponding reaction
249 mechanisms

Oxidant	Proposed reaction mechanisms
O ₃	Addition, H-atom transfer, e ⁻ -transfer, O-transfer
HOCl	Cl ⁺ -transfer, e ⁻ -transfer
Cl ₂ O	Cl ⁺ -transfer, e ⁻ -transfer
HOBr	Br ⁺ -transfer, e ⁻ -transfer
ClO ₂	e ⁻ -transfer
[•] OH	Addition, H-atom transfer, e ⁻ -transfer
Fe(VI)	e ⁻ -transfer, addition, oxygen-transfer
¹ O ₂	Addition

250

251 Table 3: Feasibility of PES computations to identify transition structures

Mechanism	PES / minimum energy path
Addition	Yes
(Heavy) atom transfer (Cl ⁺ , Br ⁺ , O [•])	Yes
H-atom transfer	Yes (if proton and electron are transferred simultaneously)
e ⁻ -transfer	No (including proton-coupled electron transfer and similar)

252

253

254 **Kinetics of reactions: Second-order rate constants k**

255 Kinetic experiments for a bimolecular reaction between a target compound (Red) and
 256 an oxidant (Ox) measure an apparent second-order rate constant k_{app} (M⁻¹s⁻¹, typically
 257 determined at 298K and 1atm), which is a lump sum of different microscopic
 258 reactivities (eq. 2):

$$259 \quad -\frac{d}{dt}[Red] = k_{app}[Red_{tot}][Ox_{tot}] = \sum_i^n \sum_j^m \sum_l^o k_{ijl}[Red_i][Ox_j] \quad (2)$$

260 where “tot” signifies total concentrations. The triple summation corresponds to (*i*)
 261 speciation in the target compound, (*j*) speciation in the oxidant, and (*l*) different
 262 reaction channels for a species-specific reaction. Therefore, k_{ijl} is a microscopic rate
 263 constant specific to a certain *i-j* species pair and a channel *l*. Simulated rate constants
 264 are computed from a specific molecular geometry, thus correspond to k_{ij} (species-
 265 specific) or k_{ijl} (channel-specific). In experiments, in contrast, pH-dependent
 266 speciation for the target compound and oxidant can be typically deconvoluted with
 267 the pK_a, while other species-specific (e.g., conformers) and channel-specific k remain
 268 indistinguishable (SI, Text S4). Therefore, a careful comparison between theoretical
 269 and experimental k is required for verification.

270

271 *ab initio* calculations of k by Transition State Theory (TST)

272 Identified transition structures allow the calculation of ΔG^\ddagger (Figure 4, right), which is
 273 linked to the rate constant through TST, using the Eyring-Polanyi equation (Table 4).
 274 Calculation of absolute microscopic rate constants requires detailed knowledge of the
 275 reaction mechanism(s)/transition structures, along with further corrections to the rate

276 expression.³¹ There are several limitations to this approach: (a) Calculations including
 277 “problematic” oxidants such as O₃ (and probably also ClO₂, Cl₂O, CO₃^{•-}) suffer from
 278 shortcomings of the used electronic structure method. (b) Ionic transition structures
 279 can be significantly stabilized by water molecules (which are lacking from the usually
 280 employed implicit solvation models) or may be catalyzed by proton transfer to and
 281 from neighboring water molecules, (c) limitations of the Eyring-Polanyi equation or
 282 similar approaches (e.g., the transmission coefficient is unknown for solution-phase
 283 reactions, and well-defined quasi-equilibria are assumed) (SI, Text S5). Estimation of
 284 $\log(k)$ close to experimental accuracy ($\sim 1 \log(k)$) would typically require an accuracy
 285 in ΔG^\ddagger of < 2 kcal/mol, which can never be warranted (Table 1). If computed and
 286 experimental $\log(k)$ differ by > 2 , this could still be due to the technical limitations of
 287 the simulation, or the rate-determining step of the reaction was not properly identified
 288 on the PES.

289 For ET reactions, transition structures are not easily identified, and rate expressions
 290 such as the Marcus or Sandros-Boltzmann equation are often used (Table 4). They
 291 express ΔG^\ddagger as a free energy difference and a fitting parameter (assumed to be
 292 constant for the studied reactions). Computational estimation of redox properties is
 293 too inaccurate^{27, 29-30} to calculate absolute rate constants.

294

295 Table 4: Simplified rate constant expressions relevant to nucleophile-electrophile
 296 interactions (SI, Text S5).

297

Eyring-Polanyi	Marcus	Sandros-Boltzmann	Klopman-Salem
$\log(k) \propto -\frac{\Delta G^\ddagger}{RT}$	$\log(k) \propto -\frac{(\lambda + \Delta G^\circ)^2}{4\lambda k_B T}$	$\log(k) \propto \frac{\Delta G + s}{RT}$	$\log(k) \propto \frac{\beta_{HOMO-LUMO}^2}{E_{HOMO,nuc} - E_{LUMO,elec}}$
ΔG^\ddagger : free energy of activation	ΔG° : difference in electrode potentials (free energy of electron transfer) λ : reorganization energy (fitting parameter in	ΔG : free energy of reaction s : fitting parameter to a set of experimental rate constants	E_{HOMO} : HOMO ^a energy on nucleophile E_{LUMO} : LUMO ^b energy on electrophile β : HOMO-LUMO resonance integral

	experimental work)		
	k_B : Boltzmann constant		

298 ^aHOMO: Highest occupied molecular orbital; ^bLUMO: Lowest unoccupied
 299 molecular orbital

300

301 *k* estimation from molecular descriptors *D*

302 A more common, pragmatic approach to estimate *k* is by regression models (e.g.,
 303 QSAR) (eq. 3):

$$304 \log(k_a) = \sum c_b \times D_{a,b} + C \quad (3)$$

305 where *k* is the second-order rate constant for the reaction between a target compound
 306 *a* and a specific oxidant, $D_{a,b}$ is the b^{th} descriptor derived from the molecular structure
 307 of the target compound *a*, c_b are coefficients fitted to experimental *k* values of a
 308 specific oxidant, and *C* is a constant. A comparison to common rate expressions
 309 (Table 4) shows that *D* has to be proportional to ΔG^\ddagger or its electrochemical
 310 formulations, irrespective of the reaction mechanism.

311

312 *Conceptual scope and limitations of QC descriptors*

313 Among different descriptors, the orbital eigenvalue of the highest occupied molecular
 314 orbital (E_{HOMO} , contained in Ψ) of the target compound is the most commonly used.
 315 This is not surprising, as it relates to all relevant rate expressions (Table 4):

316 (i) The Klopman-Salem equation describes the ease of bond-making between a
 317 nucleophile (target compound) and an electrophile (oxidant) by a donor-acceptor
 318 orbital interaction. This electron flux from the HOMO of the nucleophile to the
 319 LUMO of the electrophile is most favorable when this HOMO-LUMO energy gap is
 320 small.

321 (ii) The Marcus and Sandros-Boltzmann equations relate the rate constant of an
 322 electron transfer reaction to the free energy change and a fitting parameter (λ or *s*).
 323 The free energy change is caused by removing an electron from the target compound,
 324 and transferring it to the oxidant, corresponding to the adiabatic ionization energies
 325 (IE/oxidation potential) and electron affinities (EA/reduction potential) of the
 326 reactants (eq. 4):

$$327 \Delta G^\circ = \text{IE}(\text{reductant}) + \text{EA}(\text{oxidant}) \quad (4)$$

328 Koopmans' theorem³²⁻³³ states that the $-E_{\text{HOMO}} \cong \text{IE}$ of a molecule, and $-E_{\text{LUMO}} \cong \text{EA}$,
329 which are however vertical (non-adiabatic) quantities. In the Marcus theory, the
330 difference between vertical and adiabatic electron transfer energies is the
331 reorganization energy λ .

332 When considering a regression model of a single oxidant, its reduction potential or
333 EA remain constant, and thus any form of computed IE of the target compound can be
334 linked to electron transfer and/or bond-making reactions. Orbital energies have also
335 been used as descriptors for H-atom transfer reactions, and these can be expected to
336 be strongly correlated for a congeneric series (e.g., "phenols").³⁴ Thus, descriptors
337 related to the IE are not mechanism-specific.

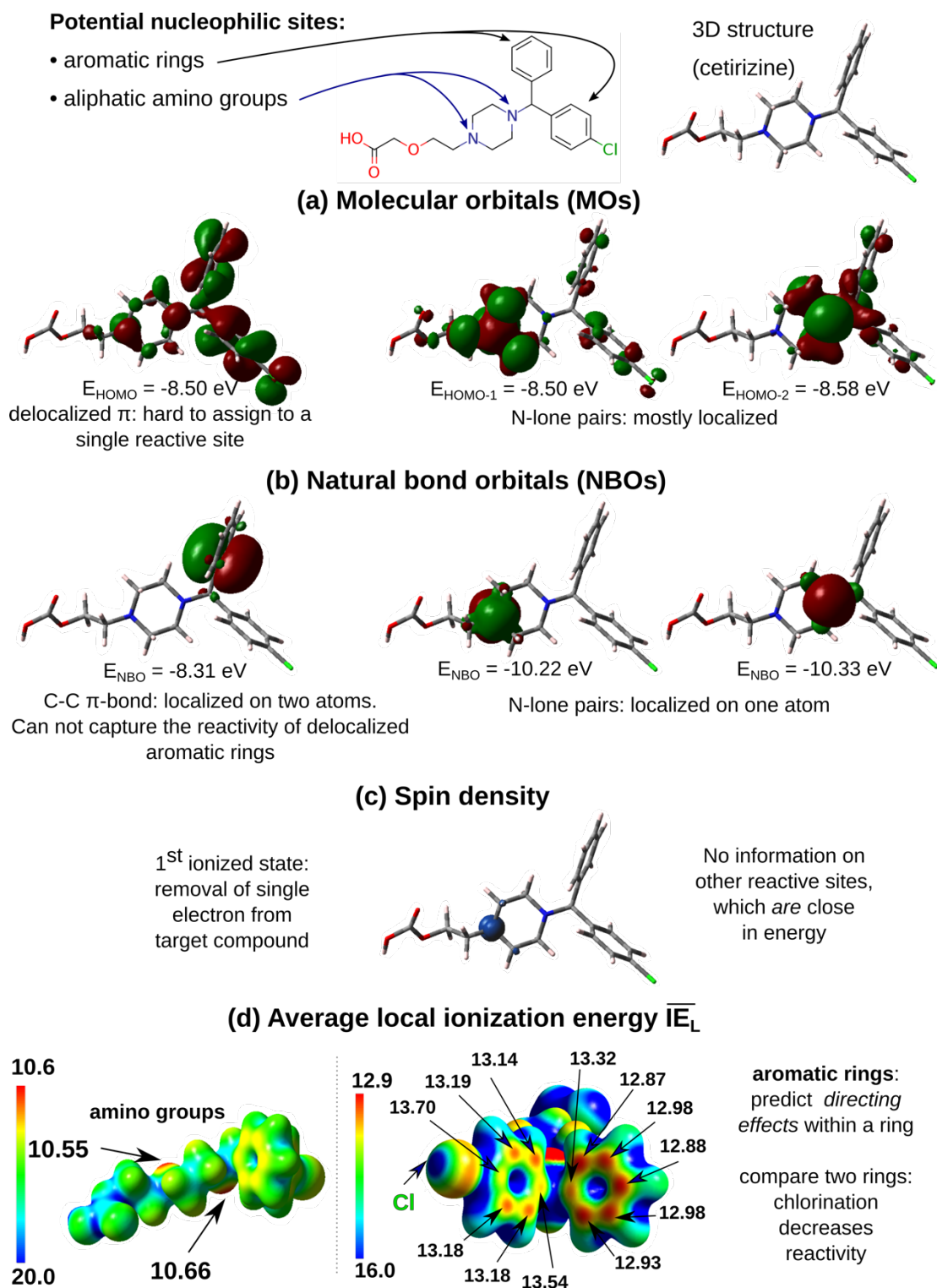
338 There are several caveats noteworthy when estimating k with QC descriptors.
339 Orbital/ionization energies cannot account for steric effects, and imply that the rate-
340 determining step of the reaction is the initial attack of the oxidant on the target
341 compound. Moreover, when considering all relevant species according to eq. 2, in
342 contrast to protonation state, conformational speciation remains undetected
343 experimentally, but can have a large impact on calculated rate constants. Figure 3a
344 shows the evolution of $-E_{\text{HOMO}}$ with the torsional angle of the methoxy group of 2,6-
345 difluoromethoxybenzene. The competition between mesomeric effects and steric
346 hinderance leads to two minima of PES that are only ~ 1.5 kcal/mol apart. However,
347 the change in $-E_{\text{HOMO}}$ is 8-fold (12 kcal/mol). Similar effects can be expected
348 whenever a torsion is associated with the disruption of mesomeric effects.
349 Consequently, algorithms that automatically generate a single guess structure for a
350 molecule have to be used cautiously (different conformations may need to be
351 considered when necessary).

352 Besides speciation, different reaction channels can contribute to the observed
353 reactivity of two well-defined species (k_{ij} vs. k_{ji}). This can refer to different
354 mechanisms (e.g., ET vs. Cl^+ -transfer, Table 2), but also a reaction at different sites
355 within an organic molecule. The used descriptors (IEs, orbital energies, bond
356 dissociation energies) are usually not mechanism-specific enough to distinguish
357 reaction channels. However, regioselectivity (different reactive sites) can be
358 described. Ψ contains descriptors to predict the likely sites of oxidation reactions in
359 target compounds. Examples beyond MOs (natural bond orbitals,³⁵ the average local
360 ionization energy IE_L ,³⁶ and the spin density of an oxidized target compound) are

361 given in Figure 5. Additionally, calculated bond dissociation energies (X-H, X=C, O,
 362 N, S, not shown) can reveal the most reactive sites for H-abstraction.

363

364



365

366 Figure 5: Insight into regioselectivity of cetirizine (SI, Text S6 for details). (a) MOs

367 are often delocalized over several reactive sites, (b) NBOs are perfectly localized on

368 one or two atoms, but fail to capture delocalization effects, (c) indicates the location

369 of the unpaired electron in a radical, (d) is a Koopmans-type ionization energy
370 projected onto a surface. Descriptors (a)-(d) predict a higher reactivity of the left
371 amino group.
372
373

374 **APPLICATION OF QUANTUM CHEMICAL COMPUTATIONS FOR**
 375 **KINETIC AND MECHANISTIC OXIDATION STUDIES**

376 **Reaction kinetics**

377 QSAR models using QC descriptors have been proposed for several oxidants (Table
 378 5).

379

380 Table 5: Examples of QSAR models for the determination of second-order rate
 381 constants that use QC descriptors.

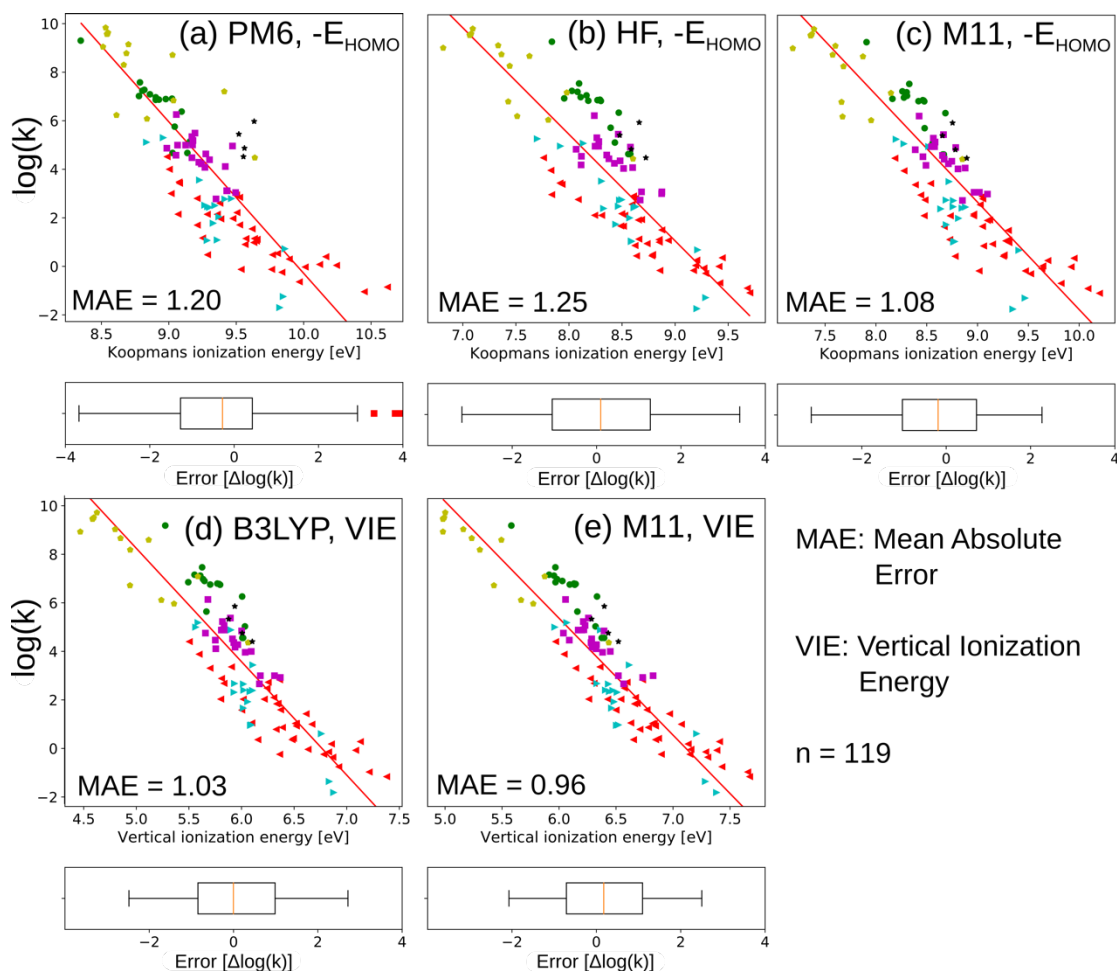
Oxidant	Target compounds	Descriptors	Rate constants
O ₃	aromatics ^{12, 37}	E_{HOMO}	k_{ij}
O ₃	olefins and amines, ¹²	E_{NBO}	k_{ij}
O ₃	phenols ³⁸	VIE ^a	k_{ij}
O ₃	aromatics ³⁷	ΔG of adduct formation	k_{ij}
HO ₂ [•] /O ₂ ⁻	various ³⁹	$E_{\text{HOMO}}/E_{\text{LUMO}}$	k_{app}
•OH	various ⁴⁰	E_{HOMO}	k_{ij}
•OH	various ⁴¹⁻⁴²	ΔG^{\ddagger} (LFER) ^b	k_{ijl}
¹ O ₂	olefins, aromatics, amines ⁴³	E_{HOMO}	k_{app}
¹ O ₂	phenols ⁴⁴	$\Delta G^{o c}$	k_{ij}
Carbonate radical	phenols, N-containing compounds ⁴⁴⁻⁴⁵	$\Delta G^{o c}$	k_{ij}
Carbon-, chlorine- and oxygen-derived radicals	various inorganic species or disproportionation ^{42, 46}	ΔG^{\ddagger} (LFER) ^b	k_{ijl}

382 ^aVIE: Vertical ionization energy, ^bLFER: Linear Free Energy Relationship, ^chalf-cell
 383 standard reduction potential

384

385 Most of the proposed correlation models used experimental k_{ij} (protonation-state
 386 specific), which collectively include all reaction channels. E_{HOMO} and E_{NBO} were

387 shown to be strongly correlated with the corresponding Hammett or Taft constants
388 from the QSAR approach,¹² wherefore these descriptors are regarded as proxies
389 reflecting the electron-donating/withdrawing effects of substituents on a reaction
390 center. Ideally, the two types of descriptors should be mutually replaceable. QC
391 descriptors yield sometimes results inferior to Hammett/Taft constants, which we
392 ascribe partly to shortcomings in the electronic structure methods used to compute
393 these descriptors. As $-E_{\text{HOMO}}$ can be interpreted as an IE, differing quality of both
394 descriptors can be expected from different methods, which is exemplified in Figure 6.
395 Systematic errors may cancel within a group of congeneric target compounds, but
396 more general models benefit from using methods that produce somewhat realistic
397 ionization/orbital energies.³³ The same argument holds for thermodynamic descriptors
398 such as bond dissociation energies or product formation energies. When considering
399 congeneric classes of compounds, QSAR-predicted rate constants agree with
400 experimental k_{ij} within a factor of 2-4.¹² However, the scope of such QSAR models is
401 limited by the structures comprised in the experimental training data set.
402 As an alternative to QSAR, absolute k computed from ΔG^\ddagger by TST were within a
403 factor of 3-750 from experimental values, depending on the oxidants, reaction types
404 and models employed.^{12, 31,41, 47}
405



406

407

408 Figure 6: Univariate QSAR models for the $\log(k)$ for the reactions between ozone and
 409 aromatic compounds. Descriptors are E_{HOMO} calculated by (a) the semi-empirical
 410 PM6 model, (b) the Hartree-Fock model, (c) the long-range corrected M11 density
 411 functional, (d) and (e) explicitly calculated VIE using B3LYP and the generally more
 412 accurate M11 functional (SI, Text S7).

413

414 **Reaction mechanisms and thermodynamic properties**

415 Mechanistic insights allow (qualitative) conclusions on the types of compounds
 416 undergoing a studied type of reaction. QC data provide information on what types of
 417 intermediates can be formed, and if they are connected on the PES. This knowledge
 418 can be used to determine the likelihood of the formation/type of transformation
 419 products (Table 6). Reaction mechanisms often involve equilibria, which can be
 420 estimated based on QC free energy calculations (Table 7).

421

422 Table 6: Illustrative examples of QC studies of oxidative reaction mechanisms

Reaction	Calculation type(s)	Gained information
<i>N,N</i> -dimethylsulfamide + O ₃ ⁴⁷	$\Delta G/\Delta G^\ddagger$	Verification/understanding of Br ⁻ -catalyzed mechanism
Acetone + $\cdot\text{OH}$ ⁴⁸	$\Delta G/\Delta G^\ddagger/k$ of 88 possible elementary reactions from reactants to experimentally observed products	Comparison of theoretically simulated time-dependent concentration profiles of the target substance and oxidation products with experimental observations
Ratinidine + mono-/dichloramine ⁴⁹	$\Delta G/\Delta G^\ddagger$	Proposition of nitric oxide as reactive nitrosating agent (refuted by experiment) ⁵⁰
<i>p</i> -substituted phenols + O ₃ ³⁸	$\Delta G/\Delta G^\ddagger$ of reactions following the initial addition of O ₃	Qualitative attribution of observed products to substituent-specific reaction mechanisms
Ibuprofen + $\cdot\text{OH}$ ⁵¹	$\Delta G/\Delta G^\ddagger$ of primary attack	Regioselectivity/branching ratio: H-abstraction, $\cdot\text{OH}$ addition
Carbamazepine + HOCl ⁵²	$\Delta G/\Delta G^\ddagger$	Elucidation of mechanisms leading to experimentally observed products

423

424

425

426 Table 7: Illustrative examples of estimated thermodynamic data

System	Calculation types(s)	Gained information
HOCl/HOBr ²²	ΔG	Estimates of unknown equilibria between

		HOX/XOX/X ₂ (X=Cl,Br)
Halamines ⁵³	ΔG /LFER	Estimated pK _a of chlor-/bromamines
Phenols ³⁸	ΔG /LFER	Estimated pK _a of phenols
Sulfonamides ²³	ΔG /LFER	Estimated ΔG° (redox potential)

427

428 PRACTICAL IMPLICATIONS AND OUTLOOK

429 *Reaction kinetics*

430 The abatement of organic micropollutants by oxidation processes is governed by
 431 reaction kinetics. Second-order rate constants for oxidation reactions can be
 432 determined experimentally or estimated by conventional QSAR methods. Both
 433 approaches have limitations. Alternatively, QSAR-based approaches with QC
 434 descriptors or *ab initio* estimations can be applied. QSAR-type approaches provide
 435 typically reasonable results for second-order rate constants within a factor of 2-4 from
 436 measured values. This is similar to differences between experimental studies. *ab initio*
 437 calculations of *k* have shown some success for $\cdot\text{OH}$ and other radicals. The
 438 application to other oxidants is largely unexplored, deserving systematic studies, and
 439 the reasons for the poor agreement with experiments need to be elucidated.

440 QSAR models with QC descriptors have been developed for the estimation of rate
 441 constants for ozone and hydroxyl radical. For chlorine, chlorine dioxide, and ferrate
 442 (VI), QSAR models using Hammett or Taft constants were successfully developed.⁶
 443 Therefore, molecular descriptors representative of a substituent effect may manifest a
 444 close correlation with rate constants, similar to E_{HOMO} or E_{NBO} for ozone.³ A
 445 concurrent use of other QC descriptors such as bond dissociation energies could lead
 446 to multivariate models that surpass current QC-based QSARs.

447 *Formation of transformation products*

448 Prediction of transformation products formed from micropollutants during oxidative
 449 water treatment is still a challenge. *ab initio* predictions are currently not possible, but
 450 QC computations can assist predictions of transformation products on several levels:
 451 (i) Confirmation of postulated reaction products by Gibbs free energy calculations,
 452 (ii) assessment of the feasibility of postulated transient products, which are not
 453 accessible experimentally, (iii) evaluation of reaction pathways with multiple reaction
 454 channels, (iv) calculation of regioselectivity and (v) calculation of physical chemical
 455 properties (e.g., pK_a, standard reduction potentials).

456 In a recently developed pathway prediction system, reactions of organic moieties with
457 ozone from experimental studies were compiled and integrated into a software using a
458 chemoinformatics tool, applying reaction rules to predict transformation products.
459 This *in silico* prediction system also includes an option for prediction of second-order
460 reaction rate constants based on QSAR-type correlations of second-order rate
461 constants with molecular orbital energies of target substances.¹³ However, on-the-fly
462 theoretical thermodynamic computations for different reaction channels remain to be
463 implemented. They are currently limited due to the lack of a reliable and affordable
464 model chemistry/software for target substances, oxidants, intermediates, and products.

465 *Outlook*

466 Testing the thermodynamic feasibility of a proposed reaction mechanism based on
467 ΔG_{rxn} is relatively easy, and should become a standard approach whenever a
468 mechanism is proposed based on experimental results. In such analyses we need to
469 consider that intermediate steps can be endergonic, and that kinetic control of the
470 reaction may lead to the thermodynamically less favorable products.

471 Detailed mechanistic studies, including the calculation of ΔG^\ddagger , have been mostly
472 limited to hydroxyl radical, for which the chemistry is the most well-understood to
473 date. With further experimental mechanistic studies, it should be possible to gain a
474 better understanding of the reactivity of other oxidants reacting by addition or atom
475 transfer (e.g., HOCl/HOBr/Cl₂O/O₃). Moreover, theoretically proposed mechanisms
476 with ΔG^\ddagger can be further verified provided that experimental ΔG^\ddagger for the corresponding
477 reaction channel can be obtained from the temperature dependence of the reaction rate
478 (i.e., from the Arrhenius equation). Eventually, such mechanistic insight based on a
479 combined experimental and computational approach could lead to pathway prediction
480 systems that cover oxidants beyond O₃.

481 SUPPORTING INFORMATION

482 Computational details; further reading on calibration of QC methods, implicit and
483 explicit solvation models, influence of the model chemistry on mechanistic
484 calculations, speciation in reaction kinetics, rate expressions for oxidation reactions,
485 regioselectivity and (de-)localization of molecular orbitals, the reaction coordinate of
486 electron transfer reactions, multireference character and singlet diradicals; 4 Figures,
487 1 Table.

488

489 BIOGRAPHICAL INFORMATION

490
491 **Peter R. Tentscher** received a PhD in chemistry from EPFL, The Swiss Federal
492 Institute of Technology, Lausanne, followed by post-doctoral stays at EPFL and
493 Eawag. He is currently a visiting scientist at Aalborg University. His research
494 interests are in computational chemistry and aqueous oxidation chemistry.

495 **Minju Lee** received a PhD in environmental chemistry from EPFL and is currently a
496 postdoctoral fellow at the University of Washington supported by the Swiss National
497 Science Foundation Early Postdoc.Mobility fellowship, investigating the application
498 of 3D-printed microfluidics for chemistry of oxidation processes.

499 **Urs von Gunten** received a PhD in Chemistry from the ETH, the Swiss Federal
500 Institute of Technology in Zurich and is currently a full professor at EPFL and a
501 senior researcher at Eawag, the Swiss Federal Institute of Aquatic Science and
502 Technology. His main interests are kinetic and mechanistic studies of disinfection and
503 abatement of micropollutants during oxidative processes.

504

505 REFERENCES

506

507

- 508 1. von Gunten, U., Oxidation Processes in Water Treatment: Are We on
509 Track? *Environmental Science & Technology* **2018**, *52*, 5062-5075.
- 510 2. NDRL/NIST Solution Kinetics Database on the Web.
511 <http://kinetics.nist.gov/solution/>.
- 512 3. von Sonntag, C.; von Gunten, U., *Chemistry of ozone in water and*
513 *wastewater treatment. From basic principles to applications*. IWA: London, 2012.
- 514 4. Deborde, M.; von Gunten, U., Reactions of chlorine with inorganic and
515 organic compounds during water treatment - Kinetics and mechanisms: A critical
516 review. *Water Research* **2008**, *42*, 13-51.
- 517 5. Heeb, M. B.; Criquet, J.; Zimmermann-Steffens, S. G.; von Gunten, U.,
518 Oxidative treatment of bromide-containing waters: Formation of bromine and its
519 reactions with inorganic and organic compounds — A critical review. *Water*
520 *Research* **2014**, *48*, 15-42.
- 521 6. Hoigné, J.; Bader, H., Kinetics of reactions of chlorine dioxide (OCLO) in
522 water - I. Rate constants for inorganic and organic compounds. *Wat. Res.* **1994**,
523 *28*, 45-55.
- 524 7. Sharma, V. K.; Zboril, R.; Varma, R. S., Ferrates: Greener Oxidants with
525 Multimodal Action in Water Treatment Technologies. *Accounts of Chemical*
526 *Research* **2015**, *48*, 182-191.
- 527 8. Waldemer, R. H.; Tratnyek, P. G., Kinetics of Contaminant Degradation by
528 Permanganate. *Environmental Science & Technology* **2006**, *40*, 1055-1061.
- 529 9. Guan, X. H.; He, D.; Ma, J.; Chen, G. H., Application of permanganate in the
530 oxidation of micropollutants: a mini review. *Frontiers of Environmental Science &*
531 *Engineering in China* **2010**, *4*, 405-413.

- 532 10. Lee, Y.; von Gunten, U., Quantitative structure-Activity relationships
533 (QSARs) for the transformation of organic micropollutants during oxidative
534 water treatment. *Water Research* **2012**, *46*, 6177-6195.
- 535 11. Minakata, D.; Li, K.; Westerhoff, P.; Crittenden, J., Development of a Group
536 Contribution Method To Predict Aqueous Phase Hydroxyl Radical (HO center
537 dot) Reaction Rate Constants. *Environmental Science & Technology* **2009**, *43*,
538 6220-6227.
- 539 12. Lee, M.; Zimmermann-Steffens, S. G.; Arey, J. S.; Fenner, K.; von Gunten, U.,
540 Development of Prediction Models for the Reactivity of Organic Compounds with
541 Ozone in Aqueous Solution by Quantum Chemical Calculations: The Role of
542 Delocalized and Localized Molecular Orbitals. *Environmental Science &*
543 *Technology* **2015**, *49*, 9925-9935.
- 544 13. Lee, M.; Blum, L. C.; Schmid, E.; Fenner, K.; von Gunten, U., A computer-
545 based prediction platform for the reaction of ozone with organic compounds in
546 aqueous solution: kinetics and mechanisms. *Environmental Science: Processes &*
547 *Impacts* **2017**, *19*, 465-476.
- 548 14. Guo, X.; Minakata, D.; Niu, J.; Crittenden, J., Computer-Based First-
549 Principles Kinetic Modeling of Degradation Pathways and Byproduct Fates in
550 Aqueous-Phase Advanced Oxidation Processes. *Environmental Science &*
551 *Technology* **2014**, *48*, 5718-5725.
- 552 15. Pari, S.; Wang, I. A.; Liu, H.; Wong, B. M., Sulfate radical oxidation of
553 aromatic contaminants: a detailed assessment of density functional theory and
554 high-level quantum chemical methods. *Environmental Science: Processes &*
555 *Impacts* **2017**, *19*, 395-404.
- 556 16. Yu, H.; Chen, J.; Xie, H.; Ge, P.; Kong, Q.; Luo, Y., Ferrate(vi) initiated
557 oxidative degradation mechanisms clarified by DFT calculations: a case for
558 sulfamethoxazole. *Environmental Science: Processes & Impacts* **2017**, *19*, 370-
559 378.
- 560 17. Cramer, C. J., *Essentials of Computational Chemistry*. John Wiley&Sons:
561 Chichester, England, 2004.
- 562 18. Trogolo, D.; Arey, J. S., Equilibria and Speciation of Chloramines,
563 Bromamines, and Bromochloramines in Water. *Environmental Science &*
564 *Technology* **2017**, *51*, 128-140.
- 565 19. Helgaker, T.; Jorgensen, P.; Olsen, J., *Molecular electronic-structure theory*.
566 John Wiley&Sons: Chichester, England, 2000.
- 567 20. Karton, A., Post-CCSD(T) contributions to total atomization energies in
568 multireference systems. *The Journal of Chemical Physics* **2018**, *149*, 034102.
- 569 21. Trogolo, D.; Arey, J. S.; Tentscher, P. R., Gas phase ozone reactions with a
570 structurally diverse set of molecules: barrier heights and reaction energies
571 evaluated by coupled cluster and density functional calculations. *J Phys Chem A*
572 *submitted*. **2018**.
- 573 22. Sivey, J. D.; Arey, J. S.; Tentscher, P. R.; Roberts, A. L., Reactivity of BrCl,
574 Br₂, BrOCl, Br₂O, and HOBr Toward Dimethenamid in Solutions of Bromide +
575 Aqueous Free Chlorine. *Environmental Science & Technology* **2013**, *47*, 1330-
576 1338.
- 577 23. Tentscher, P. R.; Eustis, S. N.; McNeill, K.; Arey, J. S., Aqueous Oxidation of
578 Sulfonamide Antibiotics: Aromatic Nucleophilic Substitution of an Aniline
579 Radical Cation. *Chemistry – A European Journal* **2013**, *19*, 11216-11223.

- 580 24. Goerigk, L.; Hansen, A.; Bauer, C.; Ehrlich, S.; Najibi, A.; Grimme, S., A look
581 at the density functional theory zoo with the advanced GMTKN55 database for
582 general main group thermochemistry, kinetics and noncovalent interactions.
583 *Physical Chemistry Chemical Physics* **2017**, *19*, 32184-32215.
- 584 25. Marenich, A. V.; Cramer, C. J.; Truhlar, D. G., Universal Solvation Model
585 Based on Solute Electron Density and on a Continuum Model of the Solvent
586 Defined by the Bulk Dielectric Constant and Atomic Surface Tensions. *The Journal*
587 *of Physical Chemistry B* **2009**, *113*, 6378-6396.
- 588 26. Thapa, B.; Schlegel, H. B., Improved pKa Prediction of Substituted
589 Alcohols, Phenols, and Hydroperoxides in Aqueous Medium Using Density
590 Functional Theory and a Cluster-Continuum Solvation Model. *The Journal of*
591 *Physical Chemistry A* **2017**, *121*, 4698-4706.
- 592 27. Tentscher, P. R.; Seidel, R.; Winter, B.; Guerard, J. J.; Arey, J. S., Exploring
593 the Aqueous Vertical Ionization of Organic Molecules by Molecular Simulation
594 and Liquid Microjet Photoelectron Spectroscopy. *The Journal of Physical*
595 *Chemistry B* **2015**, *119*, 238-256.
- 596 28. McKechnie, S.; Booth, G. H.; Cohen, A. J.; Cole, J. M., On the accuracy of
597 density functional theory and wave function methods for calculating vertical
598 ionization energies. *The Journal of Chemical Physics* **2015**, *142*, 194114.
- 599 29. Guerard, J. J.; Arey, J. S., Critical Evaluation of Implicit Solvent Models for
600 Predicting Aqueous Oxidation Potentials of Neutral Organic Compounds. *Journal*
601 *of Chemical Theory and Computation* **2013**, *9*, 5046-5058.
- 602 30. Guerard, J. J.; Tentscher, P. R.; Seijo, M.; Samuel Arey, J., Explicit solvent
603 simulations of the aqueous oxidation potential and reorganization energy for
604 neutral molecules: gas phase, linear solvent response, and non-linear response
605 contributions. *Physical Chemistry Chemical Physics* **2015**, *17*, 14811-14826.
- 606 31. Galano, A.; Alvarez-Idaboy, J. R., A computational methodology for
607 accurate predictions of rate constants in solution: Application to the assessment
608 of primary antioxidant activity. *Journal of Computational Chemistry* **2013**, *34*,
609 2430-2445.
- 610 32. Baerends, E. J.; Gritsenko, O. V.; van Meer, R., The Kohn–Sham gap, the
611 fundamental gap and the optical gap: the physical meaning of occupied and
612 virtual Kohn–Sham orbital energies. *Physical Chemistry Chemical Physics* **2013**,
613 *15*, 16408-16425.
- 614 33. Tsuneda, T.; Song, J.-W.; Suzuki, S.; Hirao, K., On Koopmans' theorem in
615 density functional theory. *The Journal of Chemical Physics* **2010**, *133*, 174101.
- 616 34. Zhang, H.-Y.; Sun, Y.-M.; Zhang, G.-Q.; Chen, D.-Z., Why Static Molecular
617 Parameters Cannot Characterize the Free Radical Scavenging Activity of Phenolic
618 Antioxidants. *Quantitative Structure-Activity Relationships* **2000**, *19*, 375-379.
- 619 35. Glendening, E. D.; Landis, C. R.; Weinhold, F., Natural bond orbital
620 methods. *Wiley Interdisciplinary Reviews: Computational Molecular Science* **2011**,
621 *2*, 1-42.
- 622 36. Brown, J. J.; Cockroft, S. L., Aromatic reactivity revealed: beyond
623 resonance theory and frontier orbitals. *Chemical Science* **2013**, *4*, 1772-1780.
- 624 37. Naumov, S.; von Sonntag, C., Quantum Chemical Studies on the Formation
625 of Ozone Adducts to Aromatic Compounds in Aqueous Solution. *Ozone: Science &*
626 *Engineering* **2010**, *32*, 61-65.
- 627 38. Tentscher, P. R.; Bourgin, M.; von Gunten, U., Ozonation of Para-
628 Substituted Phenolic Compounds Yields p-Benzoquinones, Other Cyclic α,β -

629 Unsaturated Ketones, and Substituted Catechols. *Environmental Science &*
630 *Technology* **2018**, *52*, 4763-4773.

631 39. Nolte, T. M.; Peijnenburg, W. J. G. M., Use of quantum-chemical descriptors
632 to analyze reaction rate constants between organic chemicals and
633 superoxide/hydroperoxyl ($O_2^{\cdot-}/HO_2^{\cdot}$). *Free Radical Research* **2018**, 1-411.

634 40. Luo, X.; Yang, X.; Qiao, X.; Wang, Y.; Chen, J.; Wei, X.; Peijnenburg, W. J. G.
635 M., Development of a QSAR model for predicting aqueous reaction rate constants
636 of organic chemicals with hydroxyl radicals. *Environmental Science: Processes &*
637 *Impacts* **2017**, *19*, 350-356.

638 41. Minakata, D.; Crittenden, J., Linear Free Energy Relationships between
639 Aqueous phase Hydroxyl Radical Reaction Rate Constants and Free Energy of
640 Activation. *Environmental Science & Technology* **2011**, *45*, 3479-3486.

641 42. Minakata, D.; Mezyk, S. P.; Jones, J. W.; Daws, B. R.; Crittenden, J. C.,
642 Development of Linear Free Energy Relationships for Aqueous Phase Radical-
643 Involved Chemical Reactions. *Environmental Science & Technology* **2014**, *48*,
644 13925-13932.

645 43. Nolte, T. M.; Peijnenburg, W. J. G. M., Aqueous-phase photooxygenation of
646 enes, amines, sulfides and polycyclic aromatics by singlet ($a^1\Delta_g$) oxygen:
647 prediction of rate constants using orbital energies, substituent factors and
648 quantitative structure–property relationships. *Environmental Chemistry* **2017**,
649 *14*, 442-450.

650 44. Arnold, W. A.; Oueis, Y.; O'Connor, M.; Rinaman, J. E.; Taggart, M. G.;
651 McCarthy, R. E.; Foster, K. A.; Latch, D. E., QSARs for phenols and phenolates:
652 oxidation potential as a predictor of reaction rate constants with
653 photochemically produced oxidants. *Environmental Science: Processes & Impacts*
654 **2017**, *19*, 324-338.

655 45. Arnold, W. A., One electron oxidation potential as a predictor of rate
656 constants of N-containing compounds with carbonate radical and triplet excited
657 state organic matter. *Environmental Science: Processes & Impacts* **2014**, *16*, 832-
658 838.

659 46. Minakata, D.; Kamath, D.; Maetzold, S., Mechanistic Insight into the
660 Reactivity of Chlorine-Derived Radicals in the Aqueous-Phase UV–Chlorine
661 Advanced Oxidation Process: Quantum Mechanical Calculations. *Environmental*
662 *Science & Technology* **2017**, *51*, 6918-6926.

663 47. Trogolo, D.; Mishra, B. K.; Heeb, M. B.; von Gunten, U.; Arey, J. S., Molecular
664 Mechanism of NDMA Formation from N,N-Dimethylsulfamide During Ozonation:
665 Quantum Chemical Insights into a Bromide-Catalyzed Pathway. *Environmental*
666 *Science & Technology* **2015**, *49*, 4163-4175.

667 48. Kamath, D.; Mezyk, S. P.; Minakata, D., Elucidating the Elementary
668 Reaction Pathways and Kinetics of Hydroxyl Radical-Induced Acetone
669 Degradation in Aqueous Phase Advanced Oxidation Processes. *Environmental*
670 *Science & Technology* **2018**, *52*, 7763-7774.

671 49. Liu, Y. D.; Selbes, M.; Zeng, C.; Zhong, R.; Karanfil, T., Formation
672 Mechanism of NDMA from Ranitidine, Trimethylamine, and Other Tertiary
673 Amines during Chloramination: A Computational Study. *Environmental Science &*
674 *Technology* **2014**, *48*, 8653-8663.

675 50. Spahr, S.; Cirpka, O. A.; von Gunten, U.; Hofstetter, T. B., Formation of N-
676 Nitrosodimethylamine during Chloramination of Secondary and Tertiary

677 Amines: Role of Molecular Oxygen and Radical Intermediates. *Environmental*
678 *Science & Technology* **2017**, *51*, 280-290.

679 51. Xiao, R.; Noerpel, M.; Ling Luk, H.; Wei, Z.; Spinney, R., Thermodynamic
680 and kinetic study of ibuprofen with hydroxyl radical: A density functional theory
681 approach. *International Journal of Quantum Chemistry* **2013**, *114*, 74-83.

682 52. Tandarić, T.; Vrček, V.; Šakić, D., A quantum chemical study of HOCl-
683 induced transformations of carbamazepine. *Organic & Biomolecular Chemistry*
684 **2016**, *14*, 10866-10874.

685 53. Heeb, M. B.; Kristiana, I.; Trogolo, D.; Arey, J. S.; von Gunten, U., Formation
686 and reactivity of inorganic and organic chloramines and bromamines during
687 oxidative water treatment. *Water Research* **2017**, *110*, 91-101.

688

689